

## Micro-PIV Measurements of In Vitro Blood Flow in a Micro-Channel

Cheol-Woo Park<sup>1</sup>¶, Sang-Joon Lee<sup>2</sup> and Sehyun Shin<sup>1</sup>

<sup>1</sup> School of Mechanical Engineering, Kyungpook National University

<sup>2</sup> Department of Mechanical Engineering, Pohang University of Science and Technology

### Abstract

Flow characteristics of blood flow in a micro channel were investigated experimentally using a micro-PIV (Particle Image Velocimetry) velocity field measurement technique. The main objective of this study was to understand the real blood flow in micron-sized blood vessels. The Reynolds number based on the hydraulic diameter of micro-channel for deionized (DI) water was about  $Re=0.34$ . For each experimental condition, 100 instantaneous velocity fields were captured and ensemble-averaged to get the spatial distributions of mean velocity. In addition, the motion of RBC (Red Blood Cell) was visualized with a high-speed CCD camera. The captured flow images of nano-scale fluorescent tracer particles in DI water were clear and gave good velocity tracking-ability. However, there were substantial velocity variations in the central region of real blood flow in a micro-channel due to the presence of red blood cells.

Key words : PIV, Micro-Channel, Blood Flow, Red Blood Cell (RBC)

### Introduction

Blood flow carries dissolved gases, nutrients, hormones, and metabolic wastes through the circulatory system in human body. It also has several important functions such as regulation of pH and ion composition of interstitial fluids, defense against toxins and pathogens, and stabilization of body temperature<sup>1</sup>. On these reasons detailed understanding of blood flow is very important in hemodynamics or hematology. Since blood flow is multi-phase, non-Newtonian as well as pulsatile in arterial vessels, it is not easy to quantify blood flow accurately regardless numerical or experimental methods, especially in vivo

case<sup>2-7</sup>.

Recently, many experimental studies measuring vascular flow have appeared that employ pulsed doppler method, ultrasonic plethysmography technique, micro-PIV and so on<sup>8-10</sup>. For example, Gijssen et al. investigated the effect of non-Newtonian properties of blood flow in a carotid bifurcation model by employing LDV and FEM (finite element method) numerical simulation<sup>11</sup>.

The entire flow field inside a micro-scale vessel is usually not easy to measure with point-wise velocity measuring instruments such as LDV and ultrasonic flow meter. In addition, most conventional flow visualization methods give only qualitative flow information. Due to rapid advances in computers,

---

¶ 1370, Sankyuk-dong, Buk-Gu, Daegu, 702-701, Korea  
E-mail : chwoopark@knu.ac.kr

optics and digital image processing techniques, instantaneous velocity fields can be extracted using a specially implemented PIV technique. Recently, the PIV method has been accepted as a reliable velocity field measurement technique<sup>12</sup>.

Flow characteristics of blood flow in micro-channels have been measured using a micro-PIV velocity field measurement technique, in particular, in the conduits of medical diagnostic chips such as lab-on-a-chip or DNA-chip<sup>13-15</sup>. With the rapid development of micro-Total Analysis System ( $\mu$ TAS) and sensitive DNA recognition technologies, it is now possible to immobilize DNA probes to small surfaces. This kind of microfluidic chips consist of many micron-sized channels for various sample tests and diagnosis<sup>14</sup>. To make optimum design of microfluidic chips, it has become even more important to understand blood flow in microchannels. The main objective of this study is to establish an experimental method to investigate blood flow containing real blood cells like RBC in micron-sized conduits.

## Experimental apparatus and Methods

In the present study, two-frame cross-correlation PIV technique was employed to measure the velocity field in a micro-channel quantitatively. The experimental setup for the micro-PIV velocity field measurements was shown in Figure 1. The PIV system consists of a cooled-CCD camera, a dual-head Nd:Yag laser, a frame grabber, a delay generator and a computer.

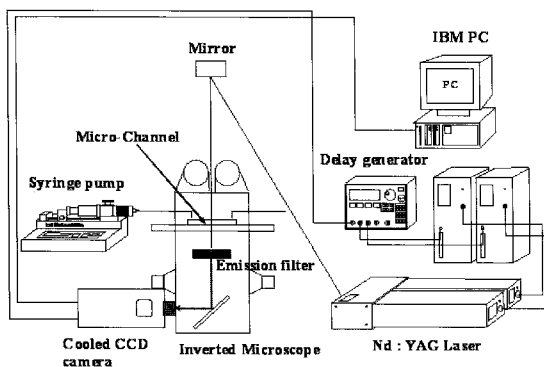


Figure 1 Schematic diagram of the micro-PIV system

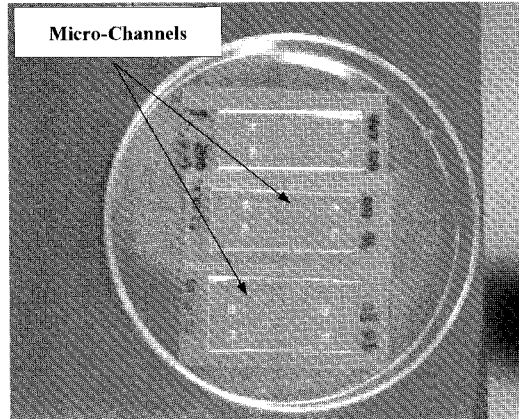


Figure 2 Photograph of micro-channels tested in this study

The CCD (SensiCam) camera with a spatial resolution of 1Kx1K pixels was used to capture particle images. The maximum energy of the two-head Nd:Yag laser is about 120mJ per pulse. The CCD camera and Nd:Yag laser were synchronized using a delay generator.

The micro-channel has rectangular cross-section of  $0.2 \times 0.04 \mu\text{m}^2$  and was installed on the stage of inverted-type microscopy. The micro-channel was made of polydimethylsiloxane (PDMS) material and a slide-glass was adhered on its top as shown in Figure 2. The fluorescent beads of 820 nm in diameter were used as seeding tracers, which excited at 532 nm wavelength and emitting the fluorescent light of 612 nm wavelength. By installing a high-pass filter of 570 nm in front of the CCD camera, clear fluorescent images can be obtained by filtering the scattering laser light effectively.

The flow image was zoomed up using a 40X lens and the interrogation window size was  $48 \times 48$  pixels and overlapped 50%. For each experimental condition, 100 instantaneous velocity fields were captured and ensemble-averaged to obtain the mean velocity field information.

In this study, we used two different working fluids; deionized (DI) water and human blood. However, for the case of human blood, we used a diluted blood solution by adding 10% of DI water in volume to get a clear flow image.

A syringe pump was used to give mean pressure-driven velocity of  $U_m = 5$  mm/s at the mid height of the channel. The corresponding Reynolds number based

on the hydraulic diameter was about  $Re=0.34$  for the case of deionized water. The flows inside the micro-channel can be assumed to be a quasi-steady laminar flow.

## Results and Discussion

### Flow Visualization

To visualize the dynamic behavior of red blood cells in a micro-channel, a high speed CCD camera of 1000 frame-rate per second was employed. Its spatial resolution is  $512 \times 512$  pixels. The field of view was zoomed to  $0.05^w \times 0.04^h$  ( $\text{mm}^2$ ) for better observation of blood cells and the depth of focus was several micrometers. The evolution of moving blood cells illuminated by halogen lamp was recorded for several seconds using the high-speed camera.

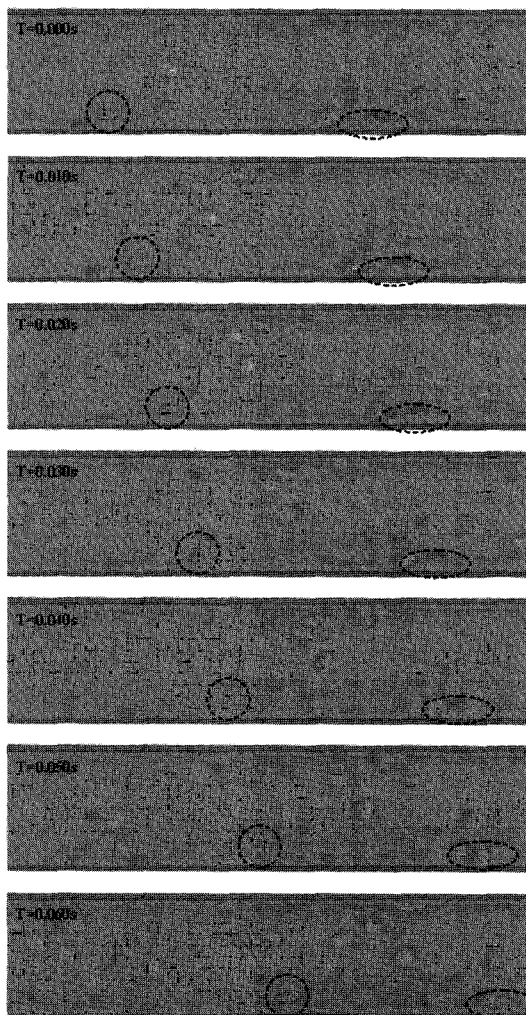


Figure 3 Evolution of red blood cells moving in a microchannel ( $W=50 \mu\text{m}$ )

Figure 3 shows the displacement of red blood cells at a 10 ms time interval. From these flow images, we can see rotation and tumbling of blood cells, and so called tank treading suspension motion. Most blood cells in the central region maintain their circular shape. Tracing the blood cell marked with a dotted circle, the RBC changes its shape according to the velocity gradient and well floats with tank treading motion with the elapse of time. This is basically attributed to the specific bi-concave shape and elastic characteristics of red blood cells.

However, the blood cell inside a dotted ellipse only shows the tumbling motion in the region near the channel wall. The blood cell also shows elastic bouncing on the channel wall with the tumbling motion as it goes downstream.

### Viscosity

The diluted blood solution tested in this study is the mixture of blood, anticoagulant material, nano-scale tracer particles and deionized water. Its viscosity was measured with a pressure-scanning capillary viscometer to compare with the unadulterated blood viscosity. In general, the flow rate and pressure drop are usually measured in conventional capillary-tube viscometry.

Figure 4 shows a schematic diagram of the modified pressure-scanning capillary viscometer (PSCV) used for viscosity measurement. It consists of a syringe, a vacuum chamber, a glass capillary tube, a receptacle,

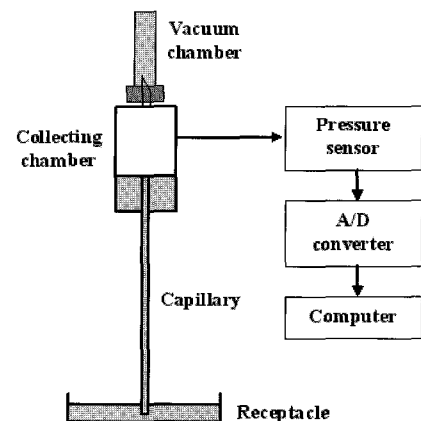


Figure 4 Schematic diagram of pressure-scanning capillary viscometer

a pressure transducer and a computer data acquisition system. The modified viscometer measures only pressure variation in the vacuum chamber and the viscosity and shear rate are directly calculated without iterative processes<sup>16</sup>. The initial volume of the vacuum chamber was  $2.5 \times 10^5 \text{ mm}^3$ . The inner diameter and length of the capillary tube were selected as  $\phi_c = 1.93 \text{ mm}$  and  $L_c = 200 \text{ mm}$  in the consideration of the friction loss in the tube that is significantly great than the other parts of the system. Capillary end effects were accounted for during data reduction by adjusting value of the length of the capillary tube.

The pressure variation inside the vacuum chamber  $P(t)$  was measured by a precision pressure transducer (Validyne DP15TL). The pressure transducer has a fast dynamic frequency response (1kHz) and a good resolution of 0.25 Pa. Furthermore, in the calibration results show an excellent linearity in the present pressure measurement range. The instantaneous pressures were recorded in a computer data file using a data acquisition system (NI DAS-16).

Prior to viscosity measurement, the atmospheric pressure ( $P_A$ ) and the total volume of the vacuum chamber ( $V_0$ ) were determined by moving the piston in the syringe to suck air from the vacuum chamber. The inner pressure of the vacuum chamber was adjusted to have a differential pressure ( $\Delta P_i = 8.6 \text{ kPa}$ ) throughout the test.

As the valve between the vacuum chamber and the capillary tube is opened, the differential pressure drives blood flow through the capillary and collected in the vacuum chamber. When the differential pressure is reduced to have a pressure head of  $\Delta P_h = 1.95 \text{ kPa}$ , the blood flow stops. A detailed description on how to derive the viscosity relation can be found in Ogawa *et al*<sup>17</sup>.

Figure 5 shows test results for a diluted human blood solution including anticoagulants and tracer particles. The blood was obtained from a healthy female donor. Viscosity was measured with varying shear rate in the range from 0.1 to 1000. The strong shear-thinning viscosity of human blood results from the presence of blood cells. However, the average

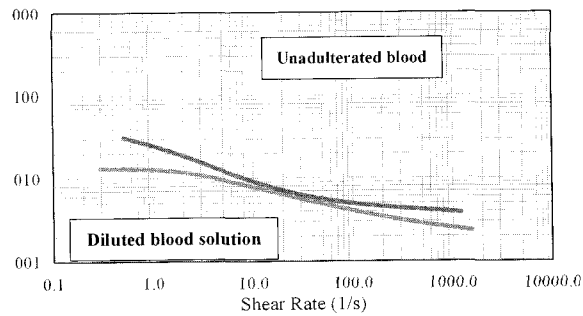


Figure 5 Comparison of viscosity as a function of shear rate

viscosity of the diluted blood solution was decreased down to a half of unadulterated real blood. From these results, we can see that the viscosity of blood flow, whether it is diluted or not, is substantially different from the constant viscosities of plasma and DI water. Since the viscosity is a function of shear rate, the blood flow in a micro-channel or blood vessels has locally different viscosity.

#### Mean Velocity Fields

Figure 6 shows the mean velocity fields and contour plots of the streamwise mean velocity component measured for two different working fluids in the horizontal plane at mid height of a micro-channel

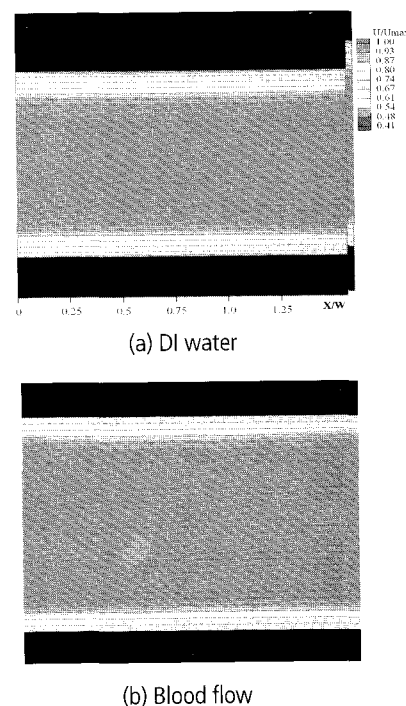


Figure 6 Mean velocity fields and contour plots of streamwise mean velocity ( $W = 200 \mu\text{m}$ )

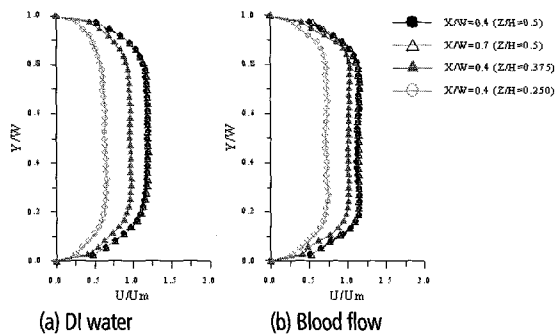


Figure 7 Mean streamwise velocity profiles at different trench heights

( $W=200\mu\text{m}$ ). For the case of pure DI water, the captured flow images of fluorescent tracer particles are clear and give a nearly uniform velocity distribution in the channel center region.

However, the diluted blood flow has some velocity variations in the central regime as shown in Figure 6(b). This seems to be attributed to the presence of cells in blood flow, mostly due to red blood cells. In addition, the blood flow has larger velocity gradient in the channel wall region compared to that of DI water.

Figure 7 shows the mean velocity profiles at three different trench heights  $Z/H=0.25, 0.375,$  and  $0.5$ . The velocity profiles at two different downstream locations in the same mid height are nearly similar and the difference in velocity magnitude is only a few.

In general, the streamwise mean velocity profile in a circular pipe has parabolic shape<sup>10</sup>. In this study, however, the velocity distribution is slightly different from that for a circular channel pipe due to different rectangular cross-section. The mean velocity profile in the central region is nearly flat and blunt due to large aspect ratio ( $W/H=5$ ) of the rectangular channel<sup>13</sup>.

However, variation of velocity profiles according to the height of measurement plane is distinguishable for two working fluids. The human blood has been known as shear-thinning fluid and most of the cells naturally migrate in the central region of blood vessels.

Therefore, the velocity of blood flow in the channel wall region at the mid height is accelerated due to the shear-thinning feature of blood and the profile has relatively blunt shape, compared to the DI water case.

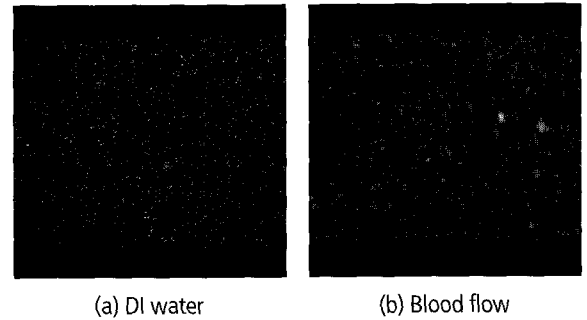


Figure 8 Raw images of fluorescent particles in DI water and diluted blood

Similarly, the same acceleration effect was observed by moving the measurement plane toward the channel wall. The mean streamwise velocity of blood flow at  $Z/H=0.25$  plane also shows large values compared to that for the DI water.

There still exist some problems in PIV measurements of two-phase blood flow. Figure 8 shows the typical raw images of fluorescent particles used for PIV measurements. Although we can extract the velocity vectors from the raw particle images, the interpolation errors will be induced by the RBC aggregation and cohesion between tracer particles and RBCs. Since the fluorescent particles were negatively charged, they were chemically reacted with RBCs and plasma after some period of time as shown in Figure 8(b).

Therefore, another elaborated method to get accurate velocity field, detecting the RBC itself and compensating the cell velocity component independently, is required to be developed.

## Conclusion

The blood flow inside a rectangular micro-channel was investigated experimentally using micro-PIV system and the results were compared with those measured for DI water under the same experimental condition. The flow structure of diluted human blood is markedly different from that of deionized water. From flow visualization experiments, we can figure out that the red blood cells maintain circular shape in the central region, however, they show rotation, tumbling and tank trading motion in the region near the channel wall.

The captured flow images of fluorescent tracer particles in DI water are clear and give good velocity tracking-ability. However, the blood flow has more or less velocity variations in the channel central region due to the presence of many RBCs in human blood.

In addition, the streamwise velocity of blood flow has larger values in the region near the channel wall due to the shear-thinning feature of blood flow and the velocity profile has relatively blunt shape compared with those for DI water.

### Acknowledgment

This research was supported by Kyungpook National University Research Fund, 2003 and authors especially thank for the help of Mr. G. B. Kim at POSTECH and Ms. Y. H. Ku at KNU.

### References

- Martini FH. *Fundamentals of Anatomy and Physiology*, Prentice Hall. 1989;641-669.
- Baaijens JPW, Van Steenhoven AA., Janssen JD. Numerical Analysis of Steady Generalized Newtonian Flow in a 2D Model of the carotid artery bifurcation. *Biorheology* 1993;30:63-74.
- Ballyk PD, Steinman DA, and Ethier CR. Simulation of Non-Newtonian Blood Flow in an end-to-side anastomosis. *Biorheology* 1994;31:565-586.
- Suh SH, Yoo SS, Roh HW. Numerical Analysis of Branch Flows for Newtonian and Non-Newtonian Fluids. *KSME J.* 1994;18(10):2762-2772.
- Wu SJ, Shung KK. Cyclic Variation of Doppler Power from Whole Blood under Pulsatile Flow. *Ultrasound in Med. & Biol.*, 1996;22(7):883-894.
- Mineshita M, Kimura T, Murai H, Moritani C, Ishioka S, Kambe M, and Yamakido M. Whole-Blood Incubation Method to Study Neutrophil Cytoskeletal Dynamics. *J. Immunol. Methods* 1997;202(1):59-66.
- Rigby GP, Ahmed S, Horseman G, and Vadgama P. In Vivo Glucose Monitoring with Open Microflow-Influences of Fluid Composition and Preliminary Evaluation in Man. *Analytica Chimica Acta*, 1991;385(1-3):23-32.
- Borg A, Fuchs L. LIF Study of Mixing in a Model of a Vein Punctured by a Cannula. *Int. J. Heat and Fluid Flow* 2002;23:664-670.
- Beach KW. Ultrasonic Measurement of Tissue Motion for the Diagnosis of Disease. *Int. J. Vascular Biomedical Eng.* 2003;1:4-12.
- Sugii Y, Nishio S, Okamoto K, Nakano A, Minamiyama M, and Niimi H. Red Blood Cell Velocity Field in Rat Mesenteric Arterioles Using Micro PIV Technique. *Int. J. Vascular Biomedical Eng.* 2003;1:24-31.
- Gijsen FJH, Van de Vosse FN, and Janssen JD. The Influence of the Non-Newtonian Properties of Blood on the Flow in Large Arteries: Steady Flow in a Carotid Bifurcation Model. *J. Biomechanics* 1999;32:601-608.
- Adrian RJ. Particle-imaging techniques for experimental fluid mechanics. *Annu. Rev. Fluid Mech.*, 1991;23:261-304.
- Meinhart CD, Wereley ST, and Santiago JG. PIV Measurements of a Microchannel Flow. *Exp. in Fluids* 1999;27:414-419.
- Shamansky LM, Davis CB, Stuart JK, Kuhr WG. Immobilization and Detection of DNA on Microfluidic Chips. *Talanta* 2001;55:909-918.
- Ernst H, Jachimowicz A, and Gerald A. High Resolution Flow Characterization in Bio-MEMS, *Sensors and Actuators A.* 2002;100:54-62.
- Shin S, Keum DY, Ku YH. Blood Viscosity Measurement Using a Pressure-Scanning Capillary Viscometer *KSME Int. J.* 2002;12:1719-1724.
- Ogawa K, Okawara S, Ito S, Taniguchi K. Blood Viscometer with Vacuum Glass Suction Tube and Needle. *J. Chemical Eng. of Japan*, 1991;24:215.